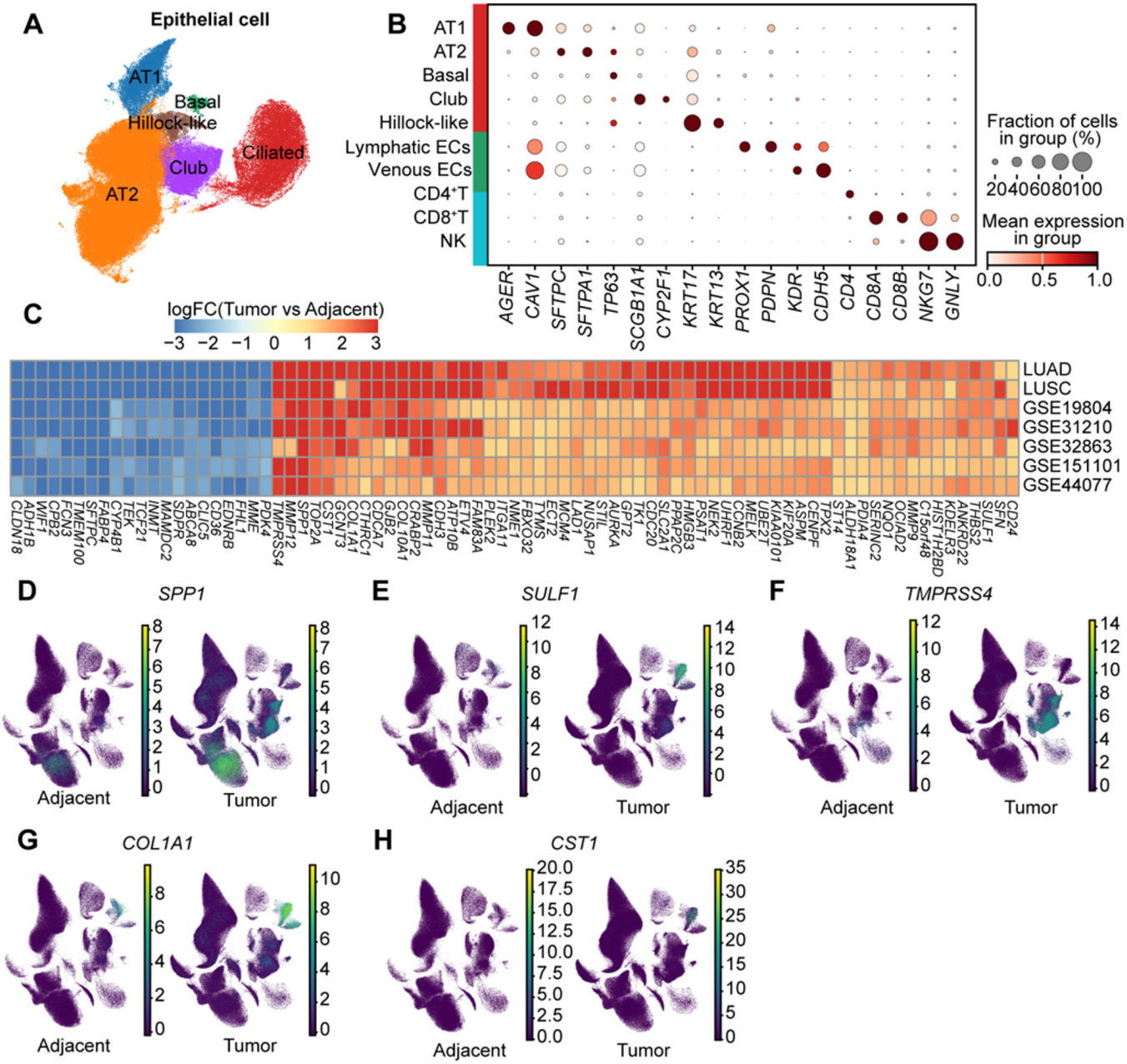

Figure S1 Distribution of differentially expressed genes in different cells. (A) UMAP visualization of Epithelial subpopulations, including AT1, AT2, Basal, Club, Hillock-like cells; (B) Dot plot depicts the expression of marker genes across different cell types in scRNA-seq data. (C) Heatmap shows the log foldchange of representative DEGs across multiple lung cancer datasets (LUAD, LUSC, GSE44077, GSE151101, GSE32863, GSE31210, and GSE19804). (D-H) Spatial transcriptomic maps illustrating the expression patterns of *SPP1*, *SULF1*, *TMPRSS4*, *COL1A1*, and *CST1* in tumor and adjacent tissues, highlighting their elevated expression in tumor regions.

https://dx.doi.org/10.21037/tlcr-2025-244

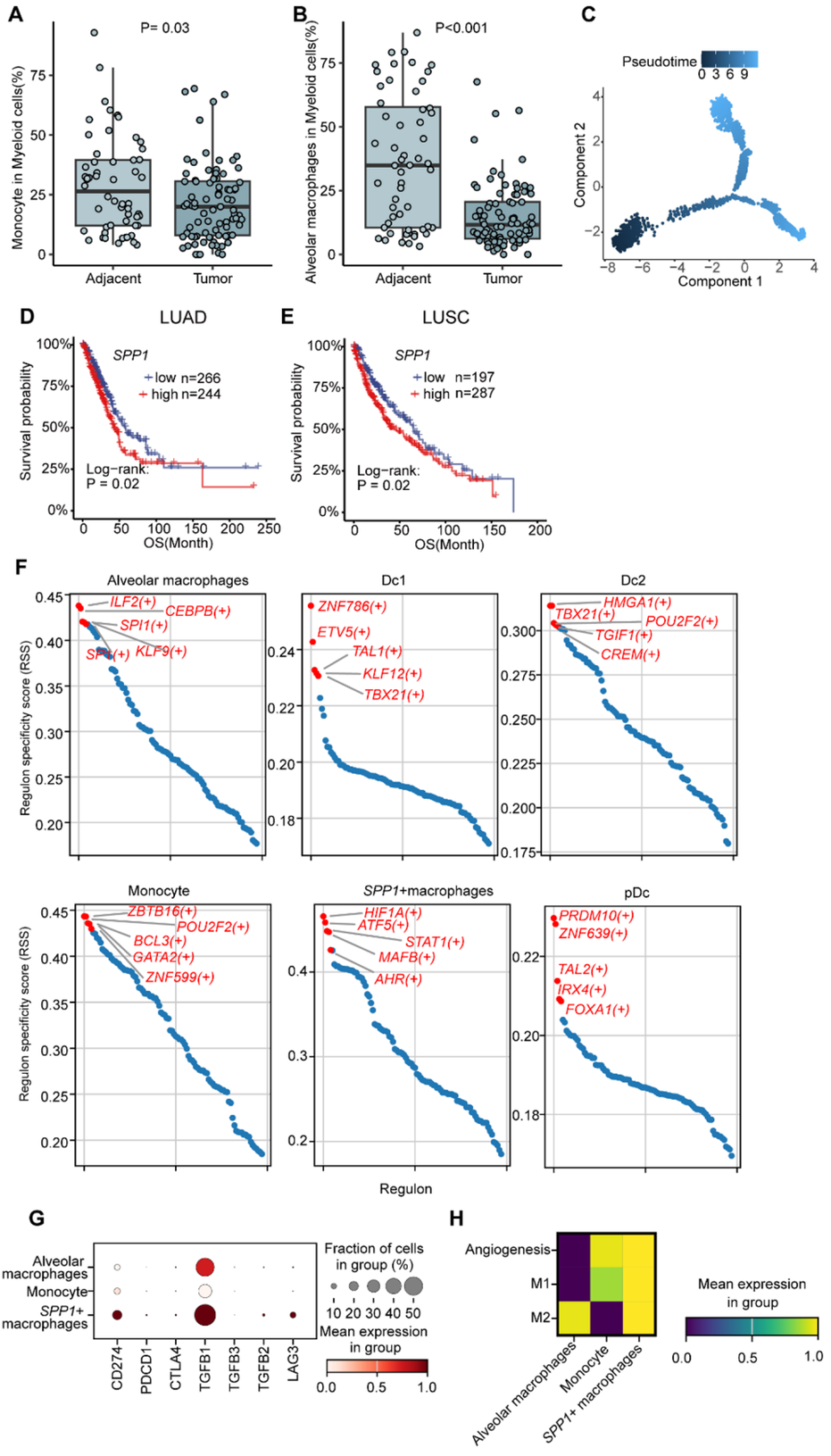

Figure S2 Regulon specificity score (RSS) of different myeloid cell subsets. (A-B). Box plots show the percentage of monocytes (A) and alveolar macrophages (B) in myeloid cells in adjacent and tumor tissues. The median, interquartile range, and outliers are indicated. (C). Pseudotime trajectory analysis of myeloid cells. (D,E) Kaplan-Meier survival analysis of overall survival (OS) based on *SPP1*$^{+}$ macrophages infiltration in LUAD (D) and LUSC (E). Statistical significance was assessed by the log-rank test. (F) Regulon specificity scores (RSS) for different myeloid cell subsets. Each panel represents a specific cell type: alveolar macrophage, DC1, DC2, monocyte, *SPP1*$^{+}$ macrophage, and pDC. The top 5 regulons with the highest RSS are highlighted in red, along with their corresponding transcription factors (TFs). The x-axis represents the regulons ranked by their RSS, and the y-axis shows the RSS values. The blue dots represent the RSS for the other regulons in each cell type. (G) Dot plot shows the expression of immunosuppressive markers across alveolar macrophages, monocytes, and *SPP1*$^{+}$ macrophages. (H) Heatmap shows the mean expression of gene signatures associated with angiogenesis, M1, and M2 polarization in alveolar macrophages, monocytes, and *SPP1*$^{+}$ macrophages.

https://dx.doi.org/10.21037/tlcr-2025-244

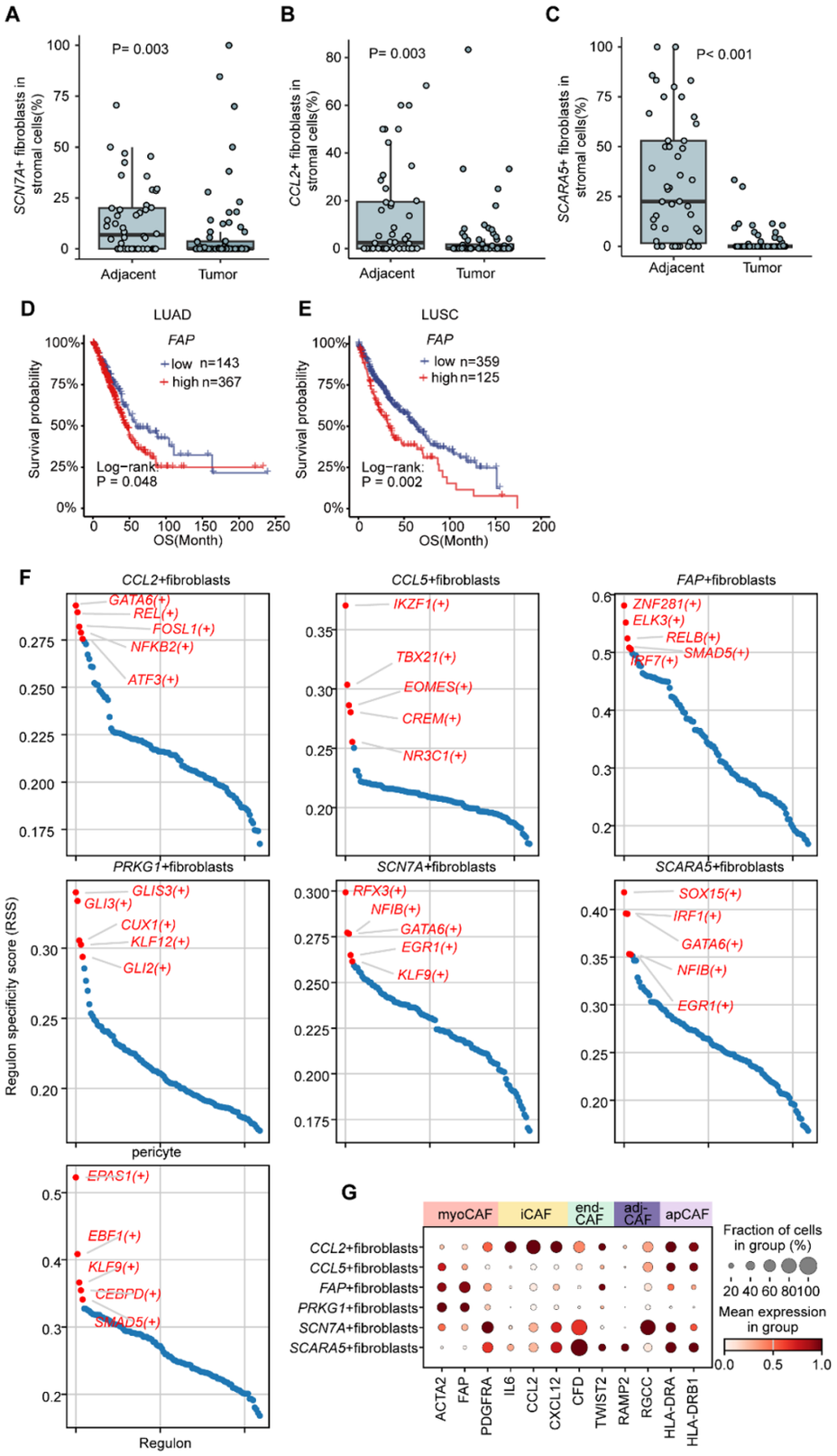

Figure S3 Regulon specificity score (RSS) of different stomal cell subsets. (A-C) Box plots compare the proportions of *FAP*$^+$ fibroblasts, *SCN7A*$^+$ fibroblasts, *CCL2*$^+$ fibroblasts and *SCARA5*$^+$ fibroblasts between adjacent and tumor tissues. Wilcoxon test p-values indicate statistical significance; (D-E) Kaplan–Meier survival analysis of overall survival (OS) based on *FAP*$^+$ fibroblasts infiltration in LUAD (D) and LUSC (E). Statistical significance was assessed by the log-rank test. (F) Each panel represents a specific cell type: *CCL2*, *CCL5*, *FAP*, *PRKG1*, *SCN7A*, and *SCARA5* fibroblasts, and pericyte. The top 5 regulons with the highest RSS are highlighted in red, along with their corresponding transcription factors (TFs). The x-axis represents the regulons ranked by their RSS, and the y-axis shows the RSS values. The blue dots represent the RSS for the other regulons in each cell type. (G) Dot plot shows the expression of representative marker genes across fibroblast subsets, including myofibroblastic CAFs (myoCAF), inflammatory CAFs (iCAF), endothelial-to-mesenchymal transition CAFs (end-CAF), adipogenic CAFs (adj-CAF), and antigen-presenting CAFs (apCAF).

https://dx.doi.org/10.21037/tlcr-2025-244

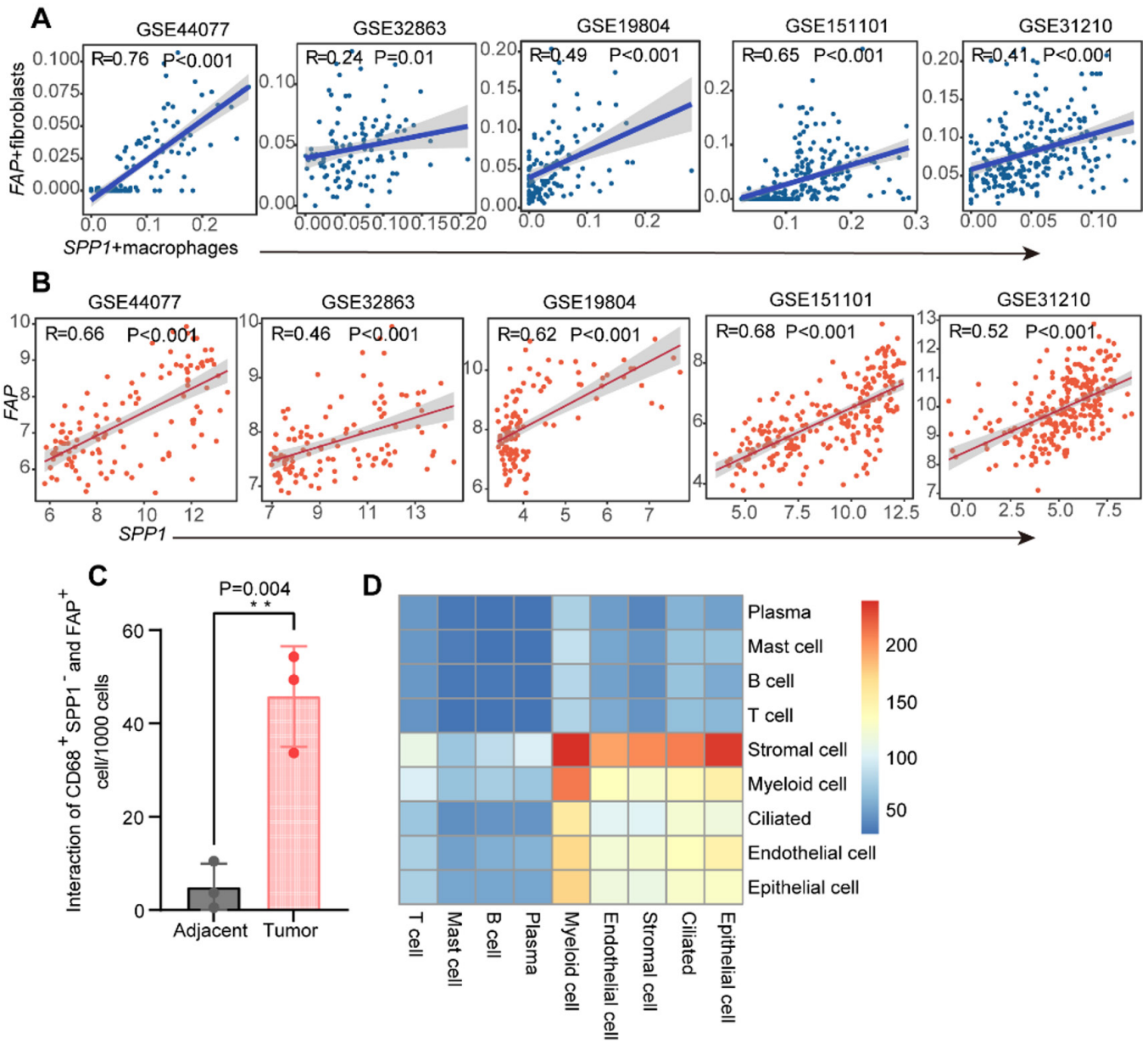

Figure S4 Correlation analysis of *SPP1*+ macrophages and *FAP*+ fibroblasts (A) Correlation between *FAP*+ fibroblast infiltration and *SPP1*+ macrophage infiltration across different datasets (GSE44077, GSE32863, GSE19804, GSE151101, GSE31210). (B) Correlation between *FAP* and *SPP1* expression across different datasets (GSE44077, GSE32863, GSE19804, GSE151101, GSE31210). (C) Statistical graph of the number of interactions between $SPP1^{-}CD68^{+}$ macrophages and FAP^{+} fibroblasts in adjacent and tumor samples of non-small cell lung cancer (n=3 samples, P=0.004; **, P<0.01; one-way ANOVA test). (D) Heatmap shows the interactions between different cell types, including T cells, mast cells, B cells, plasma cells, myeloid cells, endothelial cells, stromal cells, ciliated cells, and epithelial cells. The color intensity represents the strength of the interaction, with darker colors indicating stronger interactions. The scale on the right indicates the interaction strength values, ranging from 50 to 200.

https://dx.doi.org/10.21037/tlcr-2025-244

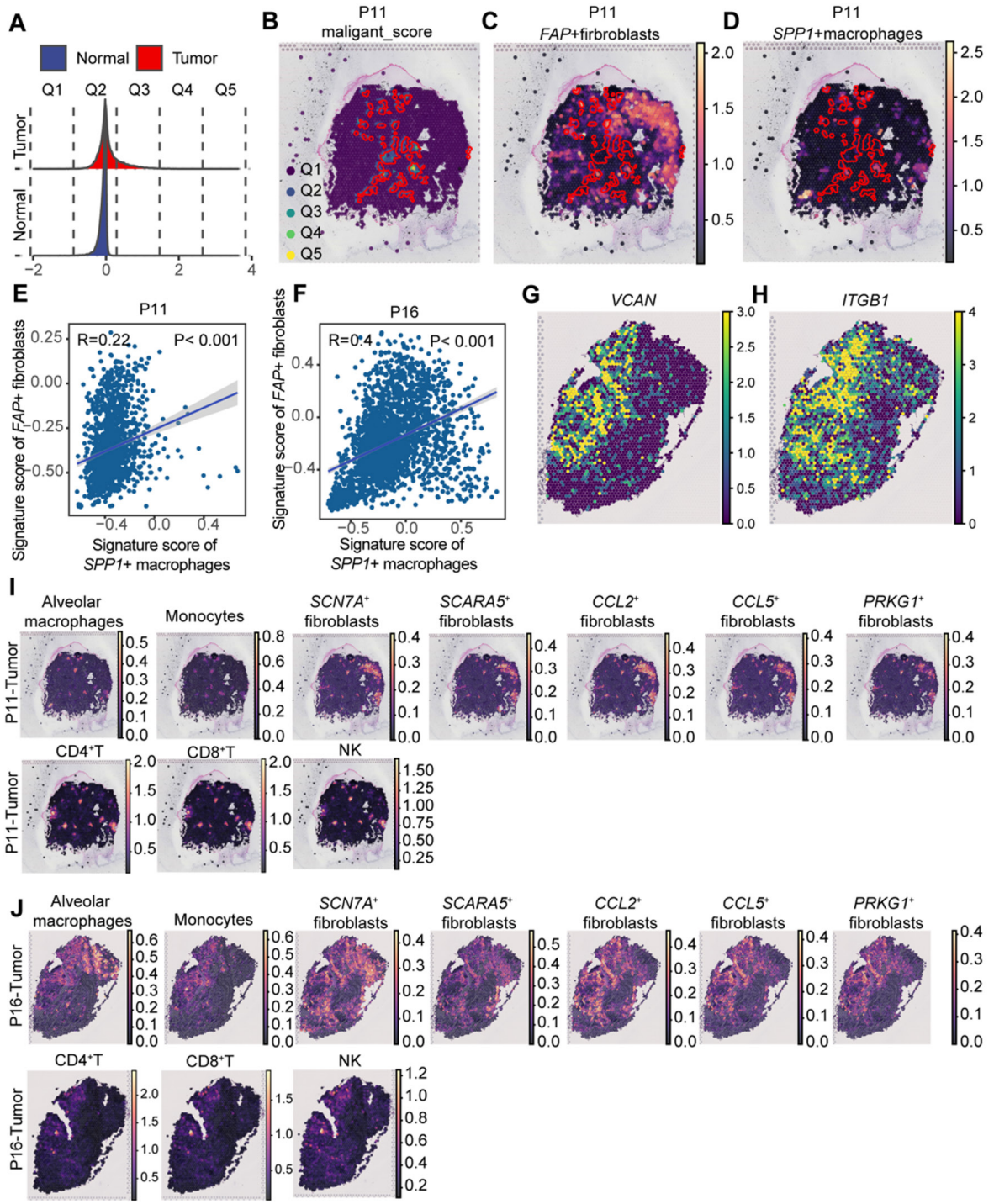

Figure S5 Co-localization of *FAP*+ fibroblasts and *SPP1*+ macrophages in NSCLC patient. (A) Distribution of malignant scores in normal and tumor regions across samples. (B) Spatial distribution of malignant score in sample P11, with tumor areas outlined and colored by malignant score quantiles (Q1–Q5). (C,D) Spatial distribution of FAP$^+$ fibroblasts (C) and SPP1$^+$ macrophages (D). (E,F) Correlation between the signature scores of *SPP1*$^+$ macrophages and *FAP*$^+$ fibroblasts in samples P11 (E) and P16 (F). Pearson's correlation coefficients (R) and p-values are shown. (G,H) Spatial expression patterns of *VCAN* (G) and *ITGB1* (H) in sample P16. (I,J) Spatial distribution of stromal and immune cells in samples P11 (I) and P16 (J), including alveolar macrophages, monocytes, fibroblast cells (*SCN7A*$^+$, *SCARA5*$^+$, *CCL2*$^+$, *CCL5*$^+$, *PRKG1*$^+$), and immune cells (CD4$^+$ T, CD8$^+$ T, NK cells).

https://dx.doi.org/10.21037/tlcr-2025-244

Table S1 Cell type-specific differentially expressed genes (DEGs) in stromal, epithelial, and myeloid cells identified from integrated scRNA-seq data

Stromal specific genes	Epithelial specific genes	Myeloid specific genes
MMP11	*TMPRSS4*	*ANKRD22*
COL10A1	*ASPM*	*MMP12*
SULF1	*ATP10B*	*C15orf48*
CTHRC1	*AURKA*	*SPP1*
COL1A1	*CCNB2*	*PLEK2*
THBS2	*CDC20*	
CST1	*CDCA7*	
ITGA11	*CDH3*	
MMP9	*CENPF*	
FBXO32	*CRABP2*	
ALDH18A1	*CTHRC1*	
KDELR3	*ECT2*	
	ETV4	
	FAM83A	
	GCNT3	
	GPT2	
	HIST1H2BD	
	HMGB3	
	KIAA0101	
	KIF20A	
	LAD1	
	MCM4	
	MELK	
	NME1	
	NQO1	
	NUSAP1	
	OCIAD2	
	PLEK2	
	PPAP2C	
	PSAT1	
	SERINC2	
	SFN	
	SLC2A1	
	ST14	
	STIL	
	TK1	
	TOP2A	
	TPX2	
	TYMS	
	UBE2T	
	UHRF1	

https://dx.doi.org/10.21037/tlcr-2025-244

Table S2 Counts of interactions between $CD68^+$ $SPP1^+$ cells and FAP^+ cells in adjacent/tumor tissues

Name	ROI	Centroid X μm	Centroid Y μm	Num Detections	Number of interaction ($CD68^+SPP1^+$ and FAP^+)	Number of interaction / 1,000 cells
Adjacent 1	Rectangle	479.51	344.47	1897	4	2.108593
Adjacent 2	Geometry	730.02	309.31	1075	4	3.72093
Adjacent 3	Polygon	665.94	112.48	477	3	6.289308
Tumor 1	Rectangle	484.01	357.95	3424	92	26.8691589
Tumor 2	Rectangle	477.52	357.95	2791	57	20.4227875
Tumor 3	Rectangle	480.51	358.45	3409	75	22.0005867

Table S3 Counts of interactions between $CD68^+$ $SPP1^-$ cells and FAP^+ cells in adjacent/tumor tissues

Name	ROI	Centroid X μm	Centroid Y μm	Num Detections	Number of interaction ($CD68^+SPP1^-$ and FAP^+)	Number of interaction/ 1,000 cells
Adjacent 1	Rectangle	479.51	344.47	1897	1	0.527148129
Adjacent 2	Geometry	730.02	309.31	1075	4	3.720930233
Adjacent 3	Polygon	665.94	112.48	477	5	10.48218029
Tumor 1	Rectangle	484.01	357.95	3424	169	49.35747664
Tumor 2	Rectangle	477.52	357.95	2791	94	33.6796847
Tumor 3	Rectangle	480.51	358.45	3409	185	54.26811382

Table S4 Quantification of $CD3^+$ and $CD8^+$ T cell proportions in *Spp1*-WT and Spp1-cKO tumor samples

Name	ROI	Centroid X μm	Centroid Y μm	Num detections	Num CD3 Opal 620	Num CD8 Opal 480	Proportion of $CD3^+$ cells in all cells	Proportion of $CD8^+$ cells in all cells	Proportion of $CD3^+$ cells in all cells(%)	Proportion of $CD8^+$ cells in all cells(%)
SPP1-WT_1	Polygon	8231.9	14753.7	6197	915	203	0.14765209	0.03275779	14.765209	3.2757786
SPP1-WT_2	Polygon	6246.5	3255.2	6720	853	49	0.12693452	0.00729167	12.693452	0.7291667
SPP1-WT_3	Geometry	8401.8	6279.5	14437	2166	141	0.15003117	0.00976657	15.003117	0.9766572
SPP1-cKO_1	Polygon	5887.4	14113.8	13087	2240	860	0.17116222	0.06571407	17.116222	6.5714067
SPP1-cKO_2	Polygon	9371.2	11825.5	20281	4136	1052	0.20393472	0.05187121	20.393472	5.187121
SPP1-cKO_3	Polygon	6502.2	3942.8	23800	4392	1044	0.18453782	0.04386555	18.453782	4.3865546

https://dx.doi.org/10.21037/tlcr-2025-244